



Contents lists available at ScienceDirect

Journal of Traditional and Complementary Medicine

journal homepage: <http://www.elsevier.com/locate/jtcme>

Inhibitory role of a smart nano-trifattyglyceride of *Moringa oleifera* root in epithelial ovarian cancer, through attenuation of FSHR - c-Myc axis



Arijit Ghosh ^{a,1}, Tanaya Roychowdhury ^{b,1}, Rajesh Nandi ^{a,1}, Rituparna Maiti ^a, Narendra N. Ghosh ^a, Sabir A. Molla ^a, Soma Mukhopadhyay ^c, Chandraday Proddhan ^d, Keya Chaudhury ^d, Priyabrata Das ^a, Nirmal K. Sarkar ^e, Samit Chattopadhyay ^f, Rittwika Bhattacharya ^{c,*}, Chinmoy K. Bose ^{c,**}, Dilip K. Maiti ^{a,***}

^a Department of Chemistry, University of Calcutta, 92 A.P.C. Road, Kolkata, 700009, India

^b Cancer Biology and Inflammatory Disorder Division, Indian Institute of Chemical Biology, 4, Raja S. C. Mullick Road, Kolkata, 700032, India

^c Department of Molecular Biology and Gynaecological Oncology, Netaji Subhas Chandra Bose Cancer Research Institute, 3081 Nayabad, Kolkata, 700094, India

^d Department of Molecular and Human Genetics, Indian Institute of Chemical Biology, 4, Raja S.C. Mullick Road, Kolkata, 700032, India

^e Department of Biological Sciences, Presidency University, 86/1, College Street Road, Kolkata, 700073, India

^f Department of Biological Sciences, BITS Pilani, K K Birla Goa Campus, India

ARTICLE INFO

Article history:

Received 9 August 2020

Received in revised form

25 March 2021

Accepted 30 March 2021

Available online 7 April 2021

Keywords:

Antitumor activity

Bioactivity guided structural identification

Mice xenograft model

Nuclear magnetic resonance

Density functional theory

Dynamic light scattering

Scanning electron microscopy

ABSTRACT

Background and aim: Epithelial ovarian cancer has the deadliest prognosis amongst gynaecological cancers, warranting an unmet need for newer drug targets. Based on its anticancer as well as abortifacient potential, *Moringa oleifera* Lam. root was hypothesized to have some implications in follicle stimulating hormone receptor (FSHR) dependent cancers like epithelial ovarian cancer.

Experimental procedure: Effect of *Moringa oleifera* Lam. root extract (MRE) was studied in epithelial ovarian cancer cell line through in vitro studies viz. MTT assay, clonogenic assay, cell cycle analysis, flow cytometry, western blot analysis, immunocytochemical analysis of FSHR and c-Myc expression and in vivo studies viz. effect of MRE in mice model of ovarian carcinoma. The structure of the active compound of MRE was elucidated following solvent extraction, purification through column chromatography, preparative TLC and bioactivity guided structural identification through ¹H-NMR, ¹³C-NMR, DEPT-135, ESIMS, FT-IR spectrophotometry, UV-vis-NIR spectrophotometry and DFT study.

Results and conclusion: Crude MRE displayed cytotoxic activity, induced apoptosis, and attenuated expression of FSHR and c-Myc in ovarian cancer cell line OAW42. MRE also attenuated expression of CD31, FSHR, and c-Myc in tumour xenograft mouse model. Finally, the active compound purified from ethyl acetate-n-hexane subfraction of MRE, that attenuated viability of ovarian carcinoma cell lines and reduced FSHR and c-Myc expression, was identified as a naturally hydrated-trifattyglyceride, showing a DFT-optimized folded amphipathic structure for easy transportation through hydrophilic and hydrophobic regions in a biological system, indicating its immense therapeutic relevance in epithelial ovarian carcinoma.

© 2021 Center for Food and Biomolecules, National Taiwan University. Production and hosting by Elsevier Taiwan LLC. This is an open access article under the CC BY-NC-ND license (<http://creativecommons.org/licenses/by-nc-nd/4.0/>).

Abbreviations: MRE, Moringa root extract; FSHR, follicle-stimulating hormone receptor; NMR, Nuclear Magnetic Resonance; DEPT, Distortionless enhancement by polarization transfer; ESI, Electrospray ionization; FT-IR, Fourier Transform Infrared Spectroscopy; UV-VIS-NIR, Ultraviolet-visible-near infrared spectroscopy; DFT, Density functional theory.

* Corresponding author.

** Corresponding author.

*** Corresponding author.

E-mail addresses: rittwika@nscir.in (R. Bhattacharya), ckbose@nscir.in (C.K. Bose), dkmchem@caluniv.ac.in (D.K. Maiti).

Peer review under responsibility of The Center for Food and Biomolecules, National Taiwan University.

¹ These authors contributed equally to this work.

<https://doi.org/10.1016/j.jtcme.2021.03.005>

2225-4110/© 2021 Center for Food and Biomolecules, National Taiwan University. Production and hosting by Elsevier Taiwan LLC. This is an open access article under the CC BY-NC-ND license (<http://creativecommons.org/licenses/by-nc-nd/4.0/>).

1. Introduction

Ovarian cancer is the seventh most common cancer in women¹ with poor prognosis, an attribute of its enigmatically complex and heterogeneous nature. Type II tumors comprising of high-grade serous carcinomas, undifferentiated carcinomas, and carcinosarcomas, are highly aggressive in nature, with a profuse expression of cytokines and/or growth factors along with gonadotrophic hormone receptors viz. follicle stimulating hormone receptor (FSHR), and G protein-coupled receptor.² Although, FSHR is mostly localized in granulosa cells of primary follicles, its overexpression in the ovarian surface epithelium and around the gonadotropin-binding sites in ovarian neoplasms strongly suggested a hormonal dependence mechanism for developing epithelial ovarian cancer.³ Overexpression of FSHR, is known to initiate and promote epithelial ovarian cancer (EOC) progression, probably through activation of various downstream effector signaling, such as c-Myc.⁴

Based on earlier studies, *Moringa oleifera* Lam., the most widely available species of the Moringaceae family, has been considered a wonder plant owing to its traditional implication as anticancer therapies as reported earlier from tropical countries.^{5–7} *Moringa oleifera* Lam. has been considered as the wonder plant, with its leaves, bark, fruit having strong anticancer effect in the breast, colorectal, oral, pancreatic, hepatocellular cancer and in melanoma.^{7–11} A single earlier report showed crude root extract nanocomposite obtained from the plant to have more efficacy than its leaves, in attenuating viability of breast, colorectal and hepatocellular carcinoma cells.¹² Based on its wide usage also as abortifacient agent¹³ we envisaged that *Moringa* root extract (MRE) might contain some active natural product that could attenuate the viability of follicular stimulating hormone receptor (FSHR) dependent cancers like epithelial ovarian epithelial cancer, preferably through FSHR antagonism.^{13–15}

In order to determine its efficacy on progression of ovarian epithelial carcinoma, our present study confirmed the presence of antiproliferative and FSHR antagonistic natural product in crude MRE, partially purified and purified active natural product. We identified the active component from *Moringa oleifera* Lam. root extract, to have a unique hydrated-trifattyglyceride structure which displayed tremendous potential for structural flexibility of its outer active nano-surface in a flip-flop mechanism towards easy transportation through hydrophilic extra and intracellular compartments as well as hydrophobic transmembrane, implicating its immense therapeutic importance.

2. Methods

2.1. Collection of the specimen

Moringa oleifera Lam. root specimens were collected from Salt Lake (Bidhan Nagar), Kolkata (22.5867° N, 88.4171° E). The plant root was authenticated at Central National Herbarium, Botanical Survey of India (Voucher No: BSI/CDM/228). The root samples were cleaned and allowed to dry completely before the preparation of the extract.

2.2. Preparation of MRE

Roots of *Moringa oleifera* Lam. were extracted in water following a, earlier protocol⁸ with little modifications. Briefly, after removal of the debris through filtration by sterile cheesecloth, one half of the crude mixture was filtered through a 0.45 µm pore sterile filter

paper into a sterile tube. For in vitro studies, the crude and filtered extracts were lyophilized and finally dissolved in DMSO at a concentration of 5 mg/mL. Filtered extract was used only for comparison with crude extract in MTT assay. The crude extract was further used for MTT assay, clonogenic assay and cell cycle assay. For making mice feed, the lyophilized crude extract was dissolved in sterile normal saline suspension at a stock concentration of 1 g/mL.

2.3. Cell culture and cell viability assay using MTT (3-(4,5-dimethylthiazole-2-yl) 2,5 diphenyl tetrazolium bromide)

Human epithelial ovarian cancer cell line OAW42 was cultured in complete DMEM Dulbecco's modified eagle medium with 10% fetal bovine serum and 1% Penicillin Streptomycin and maintained at 37°C in a humidified incubator with 5% CO₂. The cells were grown in T-25 flasks till about 80% confluence and split at a concentration of 1×10^5 cells/mL in a 96 well cell culture plate. After 24 h of growth, experimental cells were treated with variable concentrations of *Moringa* root extract (MRE) alone or in combination with Cisplatin/Paclitaxel. MTT assay was performed according to standard protocol.¹⁰ For bringing in synergistic effect in combinational treatment, the dose of individual drugs was standardized based on the combination index (CI) equation.⁸ In combinational treatment, both Cisplatin and Paclitaxel were taken at a fixed dose, sublethal to their IC-50 value (Cisplatin: dose used in combination 0.25 µM, IC-50 value: 0.35 µM; Paclitaxel: dose used in combination 0.035 nM, IC-50 value: 0.058 nM) along with a variable dose of MRE. The percentage of cell survival was calculated by $(\text{Mean OD of treated well} - \text{Mean OD of blank}) / (\text{Mean OD of control well} - \text{Mean OD of blank}) \times 100$. The drug concentration that resulted in 50% reduction of cell survival was noted as IC-50. Paclitaxel and Cisplatin at a concentration of 0.046 µM and 0.5 µM, respectively, that resulted in >50% reduction of viability of OAW42 cells (Fig. S1), were taken as positive controls. (Fig. S1).

2.4. Clonogenic assay

Clonogenic assay was performed according to established protocol^{16,17} with little modification. Briefly, OAW42 cells grown at a concentration 100 cells/flask were treated with crude lyophilized MRE at a concentration of 250 µg/mL (IC-50), at an interval of 3 days, for a total duration of 12 days. After 12 days, cells were washed with PBS, fixed with acetic acid-methanol (1:7) and finally stained with 0.5% crystal violet solution. Surviving fraction (SF) of the cells was calculated.¹⁷ Colonies of both control and treated flasks were photographed in Olympus iX72 inverted microscope.

2.5. Cell cycle analysis

OAW42 cells were serum-starved for 24 h for synchronization and then treated with MRE (IC-50 dose) for 24 h. Cell cycle analysis based on the incorporation of propidium iodide into DNA was carried out using BD Cycletest™ Plus DNA Kit, following manufacturer's instruction. Analyses of the samples were carried out flow cytometrically using BD LSR Fortessa™ TM SORP (SanJose, CA) cell analyzer and BD FACS Diva v8.0.1 software.

2.6. Western blot analysis

OAW42 cells were grown up to 70% confluency, treated with DMSO, only MRE or MRE in combination with cisplatin/paclitaxel for 24 h. Then cells were harvested. The whole cell lysate of

individual treatment groups were prepared. Expression of Caspase 9, Caspase 8, Caspase 3 and PARP1 was carried out through western blot, following established protocol.¹⁸ Antibodies were procured from Cell signaling Technology, Inc. and were used in the following dilutions: anti-caspase 9 (Mouse monoclonal, 1:1000 dil. Cat No: 9508), anti-caspase 8 (Mouse monoclonal, 1:1000 dil. Cat No. 9746), anti-caspase 3 (Rabbit polyclonal, 1:1000 dil. Cat No. 9662), anti-cleaved caspase 3 (Rabbit Polyclonal, 1:1000 dil. Cat No. 9661), anti-PARP1 (Rabbit polyclonal, 1:1000 dil. Cat No. 9541). Anti-alpha tubulin (mouse monoclonal, 1:1000 dil.) was procured from Santa Cruz Biotechnology Inc, Cat No: sc8035). Following secondary antibodies were used: HRP conjugated anti-rabbit IgG raised in Goat (Cat No. A0545, Sigma, 1:8000 dil.) and HRP conjugated anti-mouse IgG raised in Rabbit (Cat No. A9044, Sigma, 1:10,000 dil.).

2.7. Immunocytochemical study of FSHR and its downstream target c-Myc in OAW42 treated with MRE

OAW42 cells were seeded at a density of 0.6 million on coverslips in 35 mm dish in DMEM +10% FBS+1% Pen-Strep and allowed to grow overnight at 37 °C in a CO₂ incubator. The next day, cells were treated with MRE (IC-50 dosage: 250 µg/mL) with equivalent dose of DMSO as control. Immunocytochemical detection and localization of FSHR and c-Myc was carried out following reported protocol (Abcam). Scoring was done following the protocol of Perrone et al.¹⁹ Briefly, after 24hrs of treatment cells were fixed using 4% Paraformaldehyde and after PBS wash, permeabilized using 1X PBS+0.01% Triton 100 for 15min. After washing with PBS, blocking with 2% BSA in 1XPBS+0.01% Triton 100, cells were then incubated overnight with anti-FSHR (1:200; Novus Biologicals, Cat No: NBP2-36489) and anti-myc (1:200; Santa Cruz Biotechnology, Cat No: sc-789) in 1% BSA in 1XPBS+0.01% tritonX100 in a hybridization chamber at 4°C. Cells were next day washed with 1xPBS and then incubated with anti-mouse Alexa 647 (AB150115) and anti-rabbit Alexa 488 (AB150077) conjugated secondary antibodies (AbCAM) at room temperature in dark for 1 h. After washing with 1x PBS cells. Finally, coverslips were mounted on slides with Prolong Gold Antifade containing DAPI and visualized using Olympus Fluoview confocal microscope and imaged using 60X objective. Scoring was done following the protocol of Perrone et al.¹⁹

2.8. Analysis of FSHR and c-Myc transcripts in OAW42 treated with MRE

RNA extraction, semiquantitative RT-PCR to detect amplicons of FSHR and cMyc was carried out in triplicate, following previously standardized protocol.²⁰ Primers for RT-PCR (were obtained from previous reports (Table S6).^{21–23} For densitometric analysis, band intensities of candidate genes were normalized with GAPDH gene, using Image lab software, Bio-Rad. A fold change of ≥ 1.2 was considered significant.²⁴

2.9. Antitumor effect of MRE in in vivo model

Adult (8-week old) healthy Swiss albino mice were used for this study. The mice were maintained in the Department of Biological Science in Presidency University with the approval of the Institutional Animal Ethics Committee of the University that was registered with the Ministry of Environment and Forests, Government of India (Regn. No.796/03/ac/CPCSEA). All animal experiments were done following the in accordance with NIH Guide for the Care and Use of Laboratory Animal and associated guidelines. The animals were kept in polypropylene cages with sawdust litter in the animal room with regulated temperature (23 ± 2 °C) and proper light-dark cycle (12 h each Standard food pellet (Lipton Private Limited, India)

and water ad libitum were provided to the animals. The drinking water given to the mice was Gentamycin treated (0.1 µg/mL) for the study. An animal model of ovarian carcinoma was made according to the protocol of Jivrajani et al.,²⁵ using only Cyclosporin A for the development of immunocompromised mice. The mice were distributed into five groups of three each, viz. Group I: ovarian carcinoma control group [OAW42+Cyclosporin], Group II: carcinoma group with MRE treatment [OAW42+Cyclosporin A + MRE treated], Group III: Only MRE treated, Group IV: Only Cyclosporin A treated, Group V: Untreated. Briefly, after prolonged immunosuppressant treatment with Cyclosporin A (15 µg/kg body weight) for 7 days, an inoculum of OAW42 cells (5×10^6 cells/mouse in 100 µl normal saline) was injected into the ovarian bursa of Gr I and Gr II mice, either alone (Gr I) or along with oral administration of MRE (50 mg/kg body weight/mice) (Gr II). Gr III and IV mice were kept under only MRE and only Cyclosporin A treatment, respectively. Oral administration of MRE alone (Gr III) or along with intraperitoneal injection of Cyclosporin (Gr II and Gr IV), was continued for 30 days. The optimum dosages for oral or intraperitoneal administration of drugs were standardized according to organization for economic co-operation and development guidelines 423 (OECD 423) protocol. At the experimental endpoint, the sacrifice of mice, collection of ovaries, preparation of tissue block, histopathology of ovaries and immunohistochemical detection of angiogenesis marker CD31 (PECAM1), as well as FSHR and c-Myc, were carried out following our standardized protocol.²⁰

2.10. Immunohistochemical (IHC) study of expression of FSHR, c-Myc and PECAM1 (CD31) in mice model

Immunohistochemical detection of FSHR, c-MYC and angiogenesis marker PECAM1 (CD31) was carried out following our previously standardized protocol.²⁰ Scoring was done following the protocol of Perrone et al.¹⁹ Briefly, about 5 µm paraffin sections of mice ovarian tissue samples were dewaxed, rehydrated and treated overnight with primary antibodies viz. mouse anti-FSHR (NBP2-36489, Novus; dilution 1:200), anti-rabbit cMyc (sc 789, Santa Cruz; dilution 1:200) or anti-goat PECAM1 sc-1506, Santa Cruz; dilution 1:250). The slides were washed and incubated with HRP conjugated anti-mouse (NBP1-75144, Novus)/anti-rabbit (AB6721, ABCAM) (dilutions: 1:500) or anti-goat (sc-2768, Santa Cruz) (dilution: 1:500) antibodies for 1 h, washed, and developed using 3,3'-diaminobenzidine (DAB, ABCAM) as the chromogen, and counterstained with haematoxylin. Scoring was done following the protocol of Perrone et al.¹⁹ All IHC and HE stained slides were photographed in Leica DM2700 M bright field microscope.

2.11. Purification of active components of MRE through successive solvent extraction

The root of *Moringa oleifera* Lam. was extracted by Soxhlet apparatus using pure as well as a mixture of different non-polar and polar solvents such as hexane, ethyl acetate in n-hexane, ethyl acetate (5–12%) in n-hexane, methanol (2%) in ethyl acetate, methanol, and methanol in water successively. All of the extracted solvents were evaporated to dryness. All residues were tested to determine their antiproliferative effect in epithelial ovarian cancer using ovarian carcinoma cell line OAW42, OVCAR 3 through MTT assay (data not shown). Best response was obtained in ethyl acetate (5–12%)–n-hexane subfractions (F1–F5). After further purification of the subfractions (subfraction F1–F5) through column chromatography on silica gel (100–200 mesh) followed by preparative TLC, their activities were validated in ovarian carcinoma cell line OAW42 and OVCAR3 cell lines, through MTT assay, RNA and protein expression of FSHR and c-Myc. Purified subfraction that showed

best effect in vivo, was taken for characterization of the active compound by relevant spectroscopic analysis through recording $^1\text{H-NMR}$, $^{13}\text{C-NMR}$, DEPT-135, ESI-MS, FT-IR spectrophotometry, UV–vis–NIR spectrophotometry, and DFT study.

2.12. DFT study

To understand the role of the nano-trifattyglyceride. H_2O in living system, we optimized the drug geometry followed by frequency calculations with M06-2X/6-31+G(d) level of DFT theory²⁶ as implemented in Gaussian 16 software.²⁷ The solvent effect was accomplished within the framework of the integral equation formalism polarizable continuum model (IEF-PCM)²⁸ to depict the electrostatic solute–solvent interactions by the formation of a solute cavity through a series of interacting spheres.

2.13. Validation of expression of FSHR and its downstream target c-Myc in ovarian carcinoma cell line OAW42 and OVCAR3, treated with purified ethyl acetate–n-hexane subtraction

Immunocytochemical validation: The ethyl acetate–n-hexane purified subfractions (F1–F5) at their IC-50 dosage (1 $\mu\text{g/ml}$) were also validated for their effect on expression and subcellular localization of FSHR and its downstream target c-Myc, following our standardized protocol described before. Images were visualized using Olympus Fluoview confocal microscope using 60X objective. Scoring was done following the protocol of Perrone et al.¹⁹

Validation of RNA expression: After treatment with active subfraction, RNA extraction followed by semiquantitative RT-PCR was carried out in OAW42 and OVCAR3 cell line, to detect amplicons of FSHR and c-Myc (Table S1), following previously standardized protocol.^{21–23} Densitometric analysis was carried out, and the band intensities of candidate genes were normalized with the GAPDH gene, using Image lab software, Bio-Rad. A fold change of ≥ 1.2 was considered significant.²⁴

2.14. Statistical analysis

Paired *t*-test with SPSS version 16, was used to determine the difference in means of percentage survival fraction in the clonogenic assay and percentage distribution of cells in cell cycle analysis, before and after MRE treatment. One way ANOVA using SPSS version 16 was used for statistical correlation of fold change of RNA expression of FSHR and c-Myc in OAW42 with/with our MRE treatment, expression of cleaved Caspase 9, Caspase 3, PARP1, RNA expression of FSHR and c-Myc overexpression of FSHR, cMyc, and PECAM1 in different groups of mice (Gr I to V) and for pairwise comparison of alterations of nucleocytoplasmic index of ovarian tissues within groups. A nucleocytoplasmic index > 1 is considered as high following established protocol.²⁹ In all statistical analyses, for 95% confidence, and *p* value of ≤ 0.05 were considered as statistically significant.

3. Results

3.1. Antiproliferative effect of *Moringa oleifera* Lam. root extract on ovarian carcinoma

To understand the effect of MRE on OAW42 viability, roots of *Moringa oleifera* Lam. were collected, dried and grounded in sterile distilled water, stirred magnetically, filtered through a sintered, and the as-extracted water filtrate used for the following experiment. MTT assay using OAW42 revealed an IC50 value of approx. 250 $\mu\text{g/ml}$ for MRE (Fig. S1). Inhibitory effect of the root extract was more pronounced (IC-50: approx 150 $\mu\text{g/ml}$), if combined with Cisplatin

or Paclitaxel at a sublethal dose of the respective drugs (Fig. S1 and dose-response curve of Cisplatin and Paclitaxel in Fig. S2). Following the CI index calculation,⁸ low and fixed concentrations of Cisplatin and Paclitaxel were chosen to confirm the favorable synergistic action with a varying dosage of the root extract (Fig. S1). The clonogenic assay showed a significant reduction in the number of colonies in OAW42 upon treatment with the water extract (IC-50 dosage: 250 $\mu\text{g/ml}$ Fig. 1A and B). Experiments were repeated in triplicates and reproduced successfully. Flow cytometric data showed that after 24 h of treatment of OAW42 cells with *Moringa oleifera* root extract (MRE) at its IC-50 dose, DNA content progressively increased in the sub G0 phase (control: 24.1% vs treated: 39.9%; *p* < 0.05; Fig. 1C, D, E; Table S1). A significant reduction of DNA content in S phase was also observed (*p* < 0.05, Fig. 1E, Table S1). Western blotting showed that the root extract alone or in combination with Paclitaxel or with Cisplatin could significantly upregulate (*p* < 0.05) cleavage of Caspase 9 (but not Caspase 8), Caspase 3 and their downstream target PARP1 (Poly ADP Ribose Polymerase) in OAW42 cell line, indicating potential role of the MRE in induction of intrinsic apoptotic pathway. Alpha Tubulin was used as an endogenous control for normalization of fold change in expression of candidate proteins (Fig. 1F, G, H, I and J). Fold change of candidate proteins were plotted upon densitometry analysis (Fig. 1 G, H, I and J) as means \pm SEM for three independent sets of experiments. One-way ANOVA showed significant upregulation in fold change of cleaved Caspase 9, Caspase 3, PARP1 expression in only MRE, MRE with Paclitaxel and MRE with Cisplatin (*p* < 0.001) in comparison to DMSO control (Fig. 1G, I, J, Table S2).

3.2. MRE attenuated FSHR and downstream target c-Myc in ovarian carcinoma

It is revealed from the immunocytochemical (Fig. 2A and B; Table S3A), and RNA expression data (Fig. 2C and D; Table S3B) that the expression of FSHR and its downstream target c-Myc was significantly reduced (*p* < 0.05) upon treatment of MRE at its IC-50 dosage for 24 h.

3.3. MRE attenuated mouse xenograft model of ovarian carcinoma

To understand the effects of MRE on ovarian carcinoma progression in vivo, we developed an immunocompromised mouse model using adult (8 weeks old) Swiss albino mice for orthotropic xenotransplantation of human ovarian carcinoma cells utilizing Jivrajani protocol²⁵ with little modifications. Amongst the different treatment groups, the visible difference in contour and mass was observed in Gr I mice (ovarian carcinoma control group (OAW42 + Cyclosporin) compared to other groups (Fig. S3). Haematoxylin-Eosin stained mice ovary slides from the five study groups (Gr I–V) showed remarkable variations in tissue histology (Fig. 3A). Gr. I mice showed highly proliferating cells with a large nucleocytoplasmic index compared to Gr II–V (Fig. 3A). Immunohistochemical analysis of angiogenesis marker CD31 (PECAM1) showed high expression in Gr I mice, indicating profuse neovascularization (Fig. 3B) compared to other groups. One-way ANOVA result showed a significant difference in nucleocytoplasmic index between Group I and Gr II (*p* value = 0.035), Group I and Gr V (*p* value = 0.004), Gr I and Gr III (*p* = 0.004), and Gr I and Gr IV (*p* value: 0.003, Table S4). The ANOVA result also revealed a considerable difference in expression of PECAM1 between Gr I and all other groups (*p* < 0.001, Table S4). Amongst the different treatment groups, expression of FSHR was significantly high in Gr I mice, compared to Gr II–V mice (Fig. 3C). One-way ANOVA provided considerably high FSHR overexpression in Gr I mice compared to Gr II–V mice (*p* value < 0.01 in all cases) as well as Gr V (Table S4).

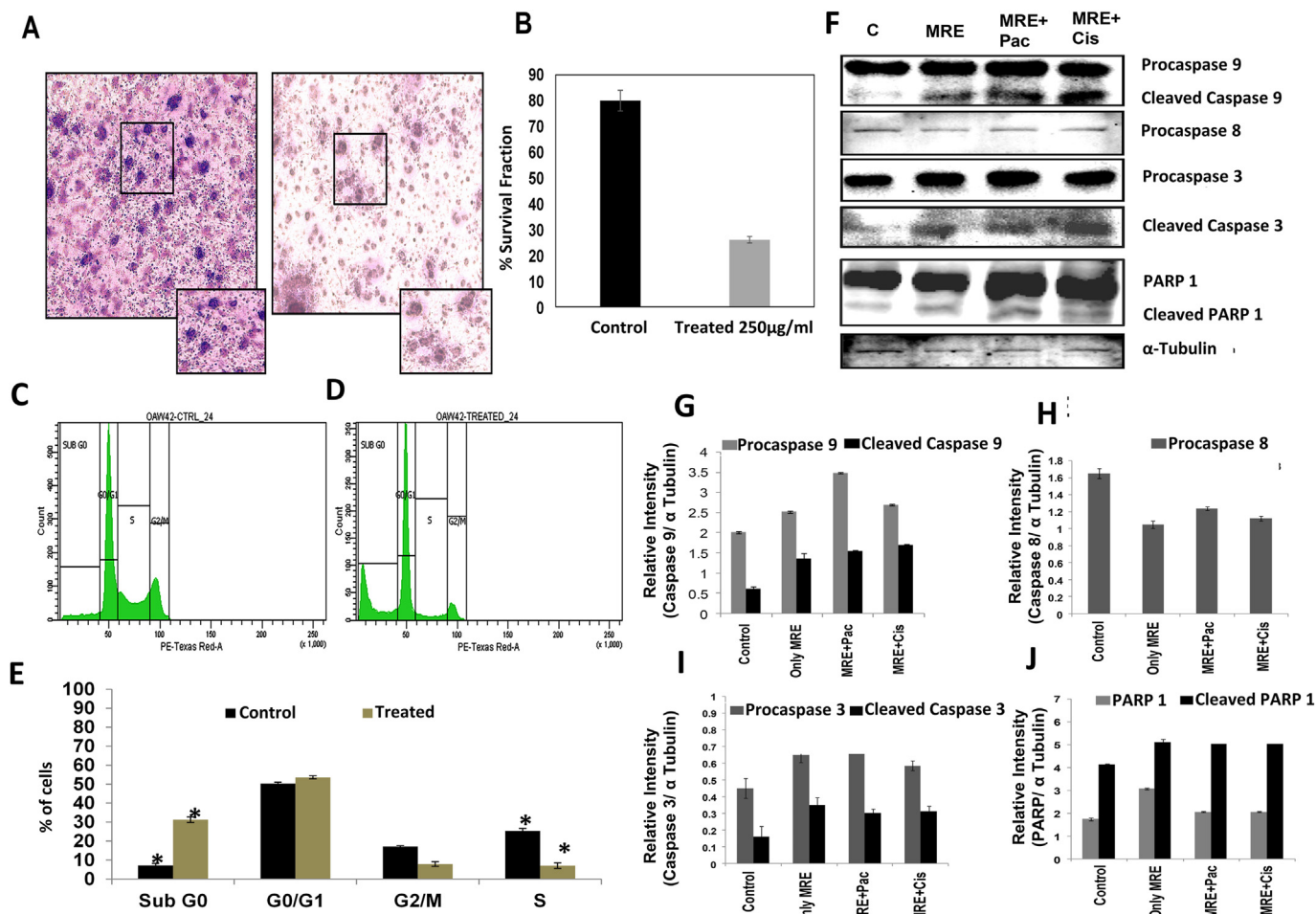


Fig. 1. In vitro study of *Moringa oleifera* Lam. root crude water extract (MRE) on survival of epithelial ovarian cancer cell line OAW42. Clonogenic assay (A, B) showed significant reduction of OAW42 colonies after treatment with 50% inhibitory concentration (IC-50: 250 µg/mL) of MRE, from data obtained from MTT cell viability assay (Fig. S1, S2). Cell cycle analysis showed a progressive increment of Propidium iodide (PI) uptake in the subG0 phase from 24 h treatment, compared to the control (C, D). Statistical significance in PI uptake is being shown as bar diagram (E). Western Blot analysis for Apoptosis assay showing significant upregulation of cleaved caspase 9, 3 and PARP1, but not Caspase8, indicating MRE induced cell death of OAW42 cells through intrinsic apoptosis mechanism (F, G, H, I and J). The normalized fold change expression of candidate proteins showing MRE alone or in combination with Paclitaxel or Cisplatin, activated Caspase 9, Caspase 3, PARP1 expression, but not Caspase 8 (F–J). One-way ANOVA for statistical difference in survival of different treatment groups is shown in Table S1, S2 (p ≤ 0.05).

Moderate to high nuclear expression of c-Myc, one important downstream target of FSHR was observed in the ovarian cortex of the carcinoma control group (Gr I). Interestingly, it was significantly reduced in Group II mice [OAW42 + MRE treated, Fig. 3d]. c-Myc expression was significantly reduced in all other groups compared to carcinoma control group (Fig. 3d; Gr III–V). However, diffused low cytoplasmic expression of c-Myc was observed in only Cyclosporin A treated group (Gr IV, Fig. 3d). One-way ANOVA showed that c-Myc overexpression was significantly high in Gr I mice compared to Gr II–V mice (p value < 0.001 in all cases, Table S4).

3.4. Isolation, bioactivity validation and purification of antiproliferative compound from MRE

Herein we aimed to identify and establish the structure of the active compound attenuating ovarian cancer progression, from MRE. The root samples were cleaned, dried, chopped, and grounded into powdery materials to extract successively in a Soxhlet apparatus using different solvent systems described before, where ethyl acetate-n-hexane subfractions showed best antiproliferative effect (data not shown). After further purification, the activities of the ethyl acetate-n-hexane subfractions (subfraction F1–F5) were

validated in ovarian carcinoma cell line OAW42 and OVCAR3 cell lines through cell viability assay (supplementary Fig. S4) as well as RNA and protein expression of FSHR and c-Myc. We found the best response of the sub-fraction eluted from ethyl acetate (10%) in n-hexane (subfraction F3 of F1–F5; now designated as TG; Fig. 4, supplementary Fig. S4, Supplementary Table S5A, B). Our immunocytochemistry data for both OAW42 (Fig. 4A) and OVCAR3 cell line (Fig. 4B), revealed that treatment groups had reduced nuclear and diffuse cytoplasmic expression of FSHR as well as c-Myc, as compared to control. In all treated groups, c-Myc expression changed from high nuclear to punctate and scattered cytoplasmic expression (Fig. 4A and B and Table S5A). The significant difference in protein expression of FSHR and c-Myc was observed in both the cell lines (Fig. 4C and D). Semi quantitative RT-PCR displayed a significant reduction of FSHR expression in OAW42, although no considerable difference in its transcript level in OVCAR3 was observed amongst treatment groups (Fig. 4E, F, G, H). The transcript level of c-Myc, an important downstream target of FSHR, was drastically reduced in both the groups (Fig. 4G and H Table S5B).

The bioactive ethyl acetate (10%) in n-hexane was further characterized through relevant spectroscopic analyses using ¹H-NMR, ¹³C-NMR, ¹³C-DEPT, ESI-MS, FT-IR, and UV–vis–NIR

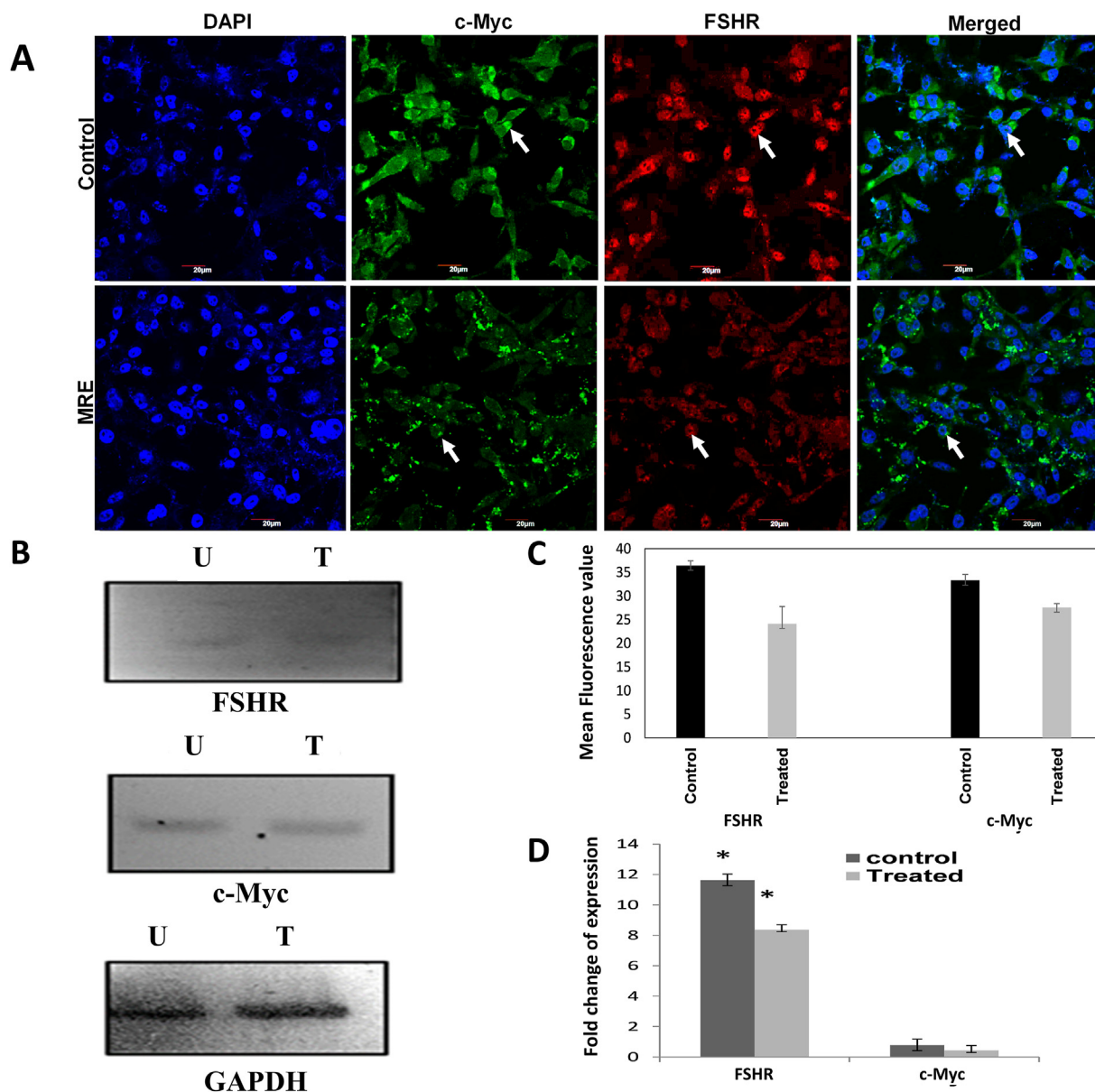


Fig. 2. Immunocytochemical (A) and RNA expression (B) analyses of FSHR and c-Myc in OAW42 cells after treatment with MRE. Data showing expression, cellular localization and Mean Fluorescence intensities (C) of FSHR and c-Myc in OAW42 cells, upon treatment of MRE (250 $\mu\text{g}/\text{mL}$ for 24 h; Magnifications 60X; Scale bar 10 μm). Densitometric fold change of expression normalized to GAPDH expression displaying significant reduction of expression of FSHR and c-Myc in MRE treated groups compared to control (D); densitometric analysis carried out using Biorad image lab software; U: untreated and T: treated for semi-quantitative RT-PCR, a fold change ≤ 1.2 considering significant. One-way ANOVA for statistical difference in survival of different treatment groups is shown Table S3 ($p \leq 0.05$). *indicating statistical significance ($p \leq 0.05$).

Spectrophotometry (Fig. 5). $^1\text{H-NMR}$ peaks at δ 5.39–5.25 region indicate the presence of olefin protons, peaks at 4.31–4.12 for O–CH₂ proton, and 2.79–0.86 for all methylene and methyl protons of linoleic and oleic acid residues (Supplementary Fig. S5). $^{13}\text{C-NMR}$ and DEPT experiments confirmed the structure along with existence of all *cis*-C=C and ester groups (Supplementary Fig. S6, S7), which were also verified by FT-IR spectroscopy (Fig. S8). The existence of water molecule in the triglyceride structure was confirmed by FTIR (3470 cm^{-1} SI), and $^1\text{H-NMR}$ (δ 7.53 and 7.72) possessing two protons of water at different chemical environments (Fig. 5A). The ESI-MS [m/z 898 (880 + 18 for water)] spectroscopic analyses confirmed the presence of water bound trifattyglyceride (Fig. 5B). It is worthy to mention that Ramsewak et al.³⁰ isolated 1, 3-dilinoleoyl-2-olein glyceride from seeds of *Dirca palustris*. Later on, Bekele and colleagues found it from roots of *Moringa stenopetala*

possessing antileishmanial bioactivity.³¹ However, the discovery of the hydrated-trifattyglyceride from *Moringa oleifera* Lam. root extract and its nanoscale dimension are unknown in the literature, which would open up new and novel opportunities for drug development.

3.4.1. Nano-scale property, DFT study, and transportation through flip-flop mechanism of hydrated trifattyglyceride

We found a major absorption bands at 362 nm of the non-aromatic compound, which indicates its existence as UV–vis active nanomaterials (Fig. 5C). The appearance of two peaks at nano-scale (33 nm, average diameter) and micron dimension (369 nm, average length) was observed in DLS (dynamic light scattering) data indicating formation of elongated nanoparticles (Fig. 5D). Gratifyingly, SEM (scanning electron microscope) imaging

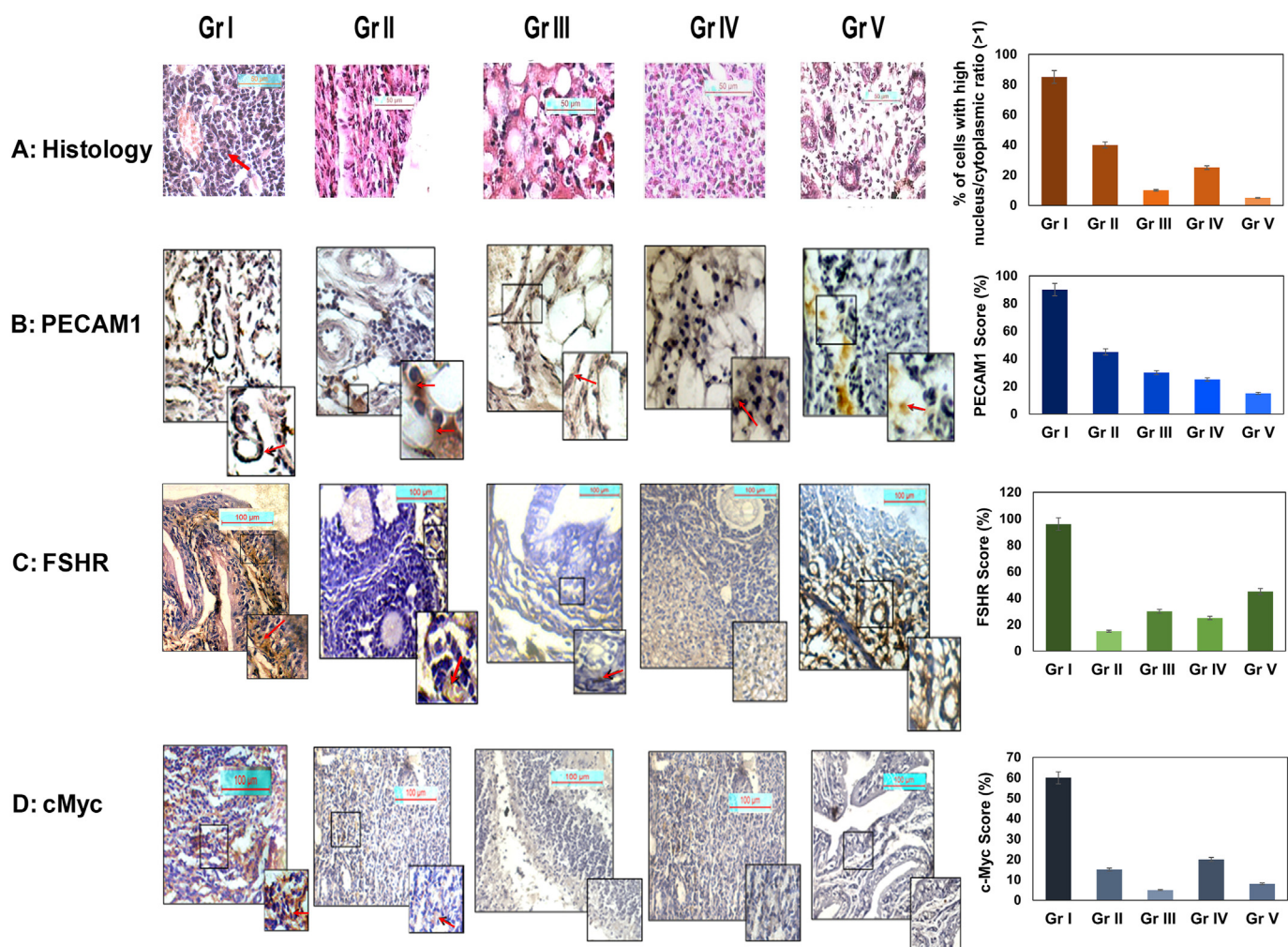


Fig. 3. In vivo study of *Moringa oleifera* Lam. root crude water extract in xenograft mice model. Haematoxyline-Eosin stained mice ovarian tissue after day 30 (A; Fig. S3), showing different treatment groups, viz. Gr I: ovarian carcinoma control [OAW42+Cyclosporin A], Gr II: carcinoma group with MRE treatment [OAW42 + Cyclosporin A + MRE treated], Gr III: only MRE treated, Gr IV: only Cyclosporin A treated, Gr V: untreated. For ovarian carcinoma control group, high nucleocytoplasmic index (black arrow) evidenced (A: Gr I); magnification 40X; scale bar: 50 μ M. Immunohistochemical localization of CD31 (PECAM1) (B), FSHR (C) and c-Myc (D) in ovarian cortex/ampulla region in ovarian carcinoma control group (Gr I) was compared with other four groups (n = 3 each). (Magnification 20X; inset 40X; scale bar 100 μ M). Arrow indicates expression. A significantly increased propensity of cells with high nucleocytoplasmic index, high expression of PECAM1, FSHR and c-Myc was evident in Gr I mice, compared to MRE treated and control groups. One-way ANOVA for statistical difference in survival of different treatment groups is shown Table S4 ($p < 0.05$)*.

of the natural product prepared by spin coating revealed the existence of spherical nanoparticles (~80 nm), which proceed for further aggregation between them to form worm-like elongated nanomaterials in micron-scale (Fig. 5E, Supplementary Fig. S9). The structure of the compound was established as a novel hydrated trifattyglyceride composed of two linoleic and oleic acid residue, namely 1,3-dilinooleyl-2-oleic glyceride (Fig. 5F). The optimized structures of the compound in the aqueous phase (Fig. 5G) displayed the clustering of water molecules around hydrophilic groups, which are exposing water surroundings leaving the hydrophobic side chains fold back. On the other hand, the hydrophilic part, along with the H-bonded water, is encapsulated in the nonpolar region by the hydrophobic long alkyl chains in the cyclohexane environment (Fig. 5H). Two hydrogen atoms of the bound water molecule to triglyceride showed non-equivalent H-bonding with distance 2.02 Å and 2.24 Å in water, and 2.22 Å and 2.28 Å in cyclohexane. This result is concordant with the experimental observation by NMR spectroscopy, which also suggests the existence of one stronger and weaker H-bonding. Furthermore, water binding is correctly found weaker in organic nonpolar

medium. Flipping of the drug molecule occurs to minimize the polar and nonpolar solvent interactions under hydrophilic (1–3, Fig. 5I) as well as hydrophobic (3–5) environment. Our DFT study indicates the immediate association of a large number of water molecules to the drug (1 → 2 or 5 → 2) on its addition to the water phase. Interestingly, release and association with water are predicted, while entering into the lipophilic cell membrane (3 → 4) and its release (4 → 5 → 2), respectively. Thus, the presence of water in the natural product trifattyglyceride plays a crucial role in the movement of the organic nanomaterials both in water (exterior and interior of cell), and hydrophobic cell membrane through a flip-flop mechanism.

As discussed earlier, our MTT-based cell survival assay and protein expression assay by immunocytochemistry showed that the active ethyl acetate-n-hexane subfraction containing the pure hydrated-triglyceride component TG (hydrated-trifattyglyceride) to be very robust in attenuating protein expression of FSHR and c-Myc in both OAW42 and OVCAR3 cell lines.

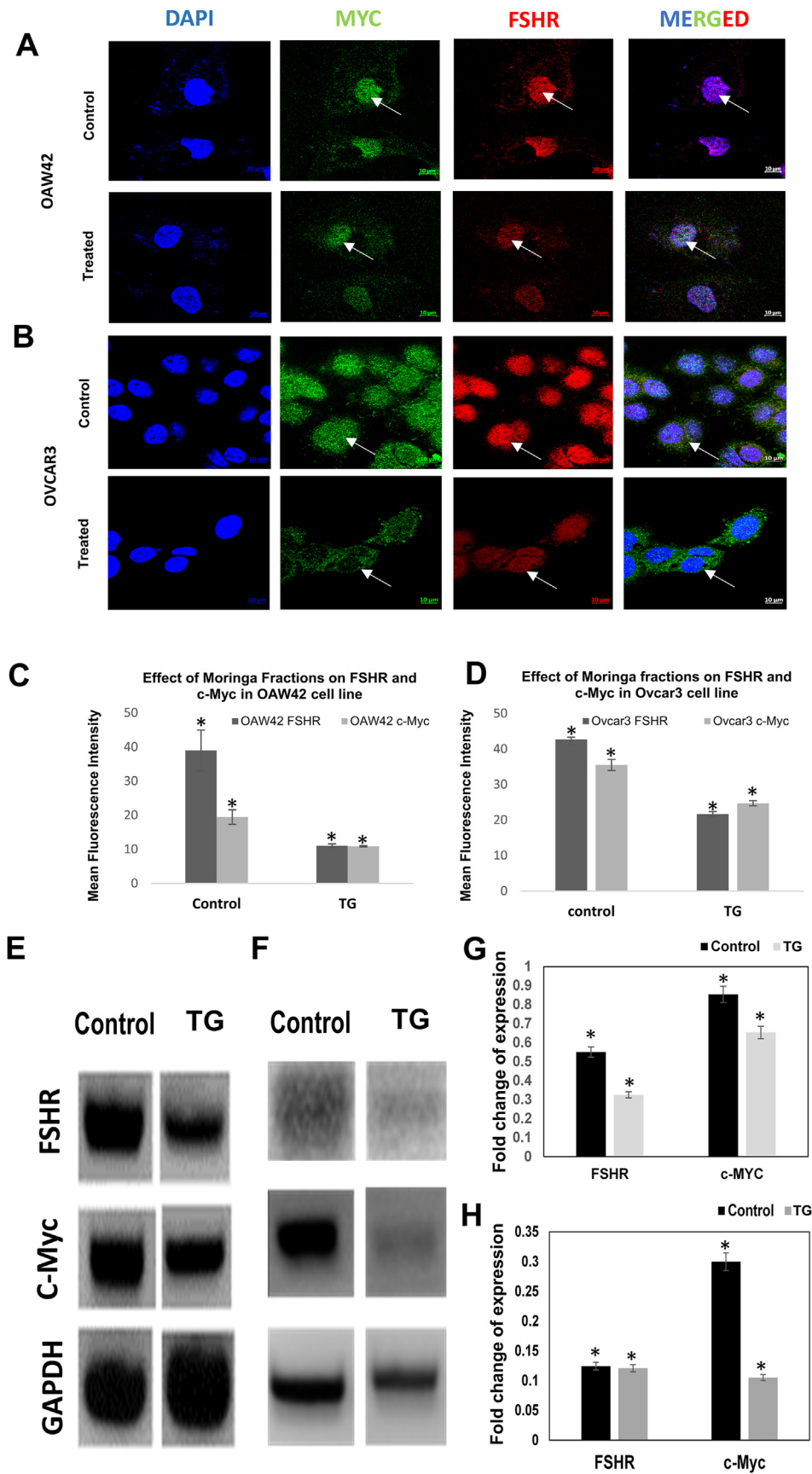


Fig. 4. Immunocytochemical and RNA expression analysis of FSHR and cMyc in OAW42 and OVCAR3 cells after treatment with purified active subfraction of MRE: Immunocytochemical analysis of FSHR and cMyc in (A) OAW42 and (B) OVCAR3 cells and their mean fluorescence intensities (C) and (D) respectively, with/without treatment with purified

4. Discussion

Epithelial ovarian cancer (EOC) has remained a major global concern owing to its intrinsic heterogeneity and therapeutic recalcitrance, with its etiology being still unknown. However, considering its unique incidence around menopause,³² Bose et al. worked on serum gonadotrophin along with inhibin etc. where significant lowering of serum FSH level was found in such EOC patients, indicating an anticipated role of gonadotrophins in development of epithelial ovarian cancer.³³ Gratifyingly, a low serum FSH level with concomitant redundant expression of FSHR on postmenopausal surface epithelium led to the development of hypothesis that an aberrant signalling network in hypothalamus-pituitary-ovarian axis, leading to overexpression of FSHR might be involved in development of EOC.³⁴ Earlier evidences found strong aberrant FSHR expression in preneoplastic ovarian surface epithelium from where EOC is supposed to originate.^{4,35}

A search for common Indian herb with anticancer potential which has significant influence on female reproductive organs led to finding *Moringa oleifera*.¹⁵ *Moringa oleifera*, which was earlier reported to have immense pharmacological implication in treating gynecological disorders³⁶ had drawn attention of investigators. Early report by Rai et al.¹⁴ and Bose³³ suggested a central antip dopamine and anti-norepinephrine and neurotrophin mediated role of MRE in mouse model. A single earlier report by Abd-Rabou et al., suggested profound anticancer effect of crude root extract nanocomposite of *Moringa oleifera* in attenuating viability of breast, colorectal and hepatocellular carcinoma cells.¹² Based on these antigonadotropic and antineoplastic and possible local and central FSHR antagonistic role of MRE, we hypothesized that MRE can be effective in FSHR dependent cancers such as epithelial ovarian cancer,⁴ as such warranting an in-depth understanding of MRE. We identified a naturally occurring nano-trifattyglyceride in MRE, which, in consensus with previous studies^{7,8,12} showed robust antiproliferative role alone and in combination with sublethal dosage of Cisplatin or Paclitaxel, attenuated anchorage-dependent colony formation ability of ovarian cancer cell line OAW42. Earlier study by Abd-Rabou et al. highlighted robust apoptosis-inducing ability of a nanocomposite formulation of the root extract of *Moringa oleifera* Lam. in the breast, colon, and hepatocellular cancer cell line,¹² although, no earlier study has hitherto identified any active compound that could attenuate ovarian cancer proliferation through FSHR antagonism.

Unlike the previous reports,⁷ our cell cycle data showed an early onset (24 h) of apoptosis upon treatment with MRE, with increment of sub G0 and G0/G1 phase. Moreover, increased Caspase 9 cleavage in a western blot of treated cells indicated the potential role of MRE in the induction of intrinsic apoptosis in epithelial ovarian cancer cell line OAW42.

In order to study the effect of MRE in mice model of ovarian carcinoma, we for the first time, developed an immunocompromised Swiss albino mice model for orthotopic xenotransplantation of OAW42 cell line, following a previously established protocol²⁵ with some modification. Our study showed that, MRE attenuated development of mice model of ovarian carcinoma through down-regulation of FSHR, c-Myc and PECAM1. Intriguingly, we observed nuclear localization of FSHR in both OAW42 and OVCAR3 cell line

but cytoplasmic in mice model. Previous reports suggested that, depending on the predominance of the splice variant, FSHR can be both cytoplasmic as well as nuclear.³⁷

Our study showed MRE not only arrested ovarian carcinoma progression but also attenuated FSHR and c-Myc transcript and protein level in both in OAW42 and mice xenograft model of ovarian carcinoma. Based on this, we hypothesized that, one FSHR antagonizing compound of MRE could play the important roles in attenuating the proliferation of ovarian epithelial carcinoma through modulation of FSHR and c-Myc signalling. Intriguingly, successive solvent extraction followed by activity assay showed robust and consistent antiproliferative efficacy in different sub-fractions (F1–F5) obtained from ethyl acetate-n-hexane solvent system. Upon further purification, the subfractions showed consistently robust antiproliferative as well as FSHR-c-Myc antagonizing effect in ovarian cancer cell lines, with maximum activity in 10% ethyl acetate-n-hexane subfraction (F3). Subfraction F3 was further characterized, and its structure was established as hydrated 1,3-dilinooleoyl-2-oleic glyceride. The spectroscopic data of the natural product is not completely the same as reported by Ramsewak³⁰ and Bekele³¹ et al. because of the associated water in it.

Effect of medium-chain fatty acid and its derivatives have earlier been suggested to have implications as antiproliferative agents on Ehrlich Ascites cancer, pancreatic cancer, glioma.^{38–40} Recent studies have shown conjugated linoleic acid (CLA) to have anti-cancer property at least in cell culture and animal models.⁴¹ Also γ -linolenic acid (GLA) and dihomo- γ -linolenic acid (DGLA), were shown to possess certain anti-cancer activities⁴² which might be relevant in this situation. Our active compound, owing to its structural flexibility of its outer active nano-surface, was suggested to transport through hydrophilic extra and intracellular compartments as well as hydrophobic transmembrane domain easily, implicating its immense therapeutic implication. A further insight into the molecular mechanism through molecular modelling or through activity assay of a synthetic derivative of the compound would enlighten our understanding of the molecular pathogenesis of MRE on ovarian epithelial cancer.

5. Conclusion

In conclusion, we demonstrated the presence of a nano-trifattyglyceride, H₂O in *Moringa oleifera* Lam. root extract to have potent antiproliferative effect and FSHR antagonistic role, implicating its immense therapeutic relevance in epithelial ovarian carcinoma. Outcome of our work has tremendous potential for development of novel therapeutic drugs for treatment of aggressive cancers like epithelial ovarian carcinoma, and it opens up new opportunities in cancer research.

Author contributions

Hypothesis that FSHR has role in etiology and progression of ovarian carcinoma and that the root of *Moringa oleifera* may contain some anticancer and antifertility agent that might have role in attenuating ovarian carcinoma was made by CKB. AG and CP conducted MTT assay, clonogenic assay, cell cycle analysis with the supervision of RB. TR performed immunocytochemistry and

active 10% ethyl acetate-n hexane subfraction of MRE (designated as TG). Magnifications 60X. Scale bar represent 10 μ m. Arrow heads indicate expression. Mean fluorescence intensity calculation showed significant reduction of expression of FSHR and c-Myc in treated cells (C, D). In treatment groups, intensity of FSHR and c-Myc was reduced, diffusely cytoplasmic and non-nucleolar. One-way ANOVA for statistical difference in survival of different treatment groups is shown in supplementary Table S5 ($p \leq 0.05$). * Indicate statistical significance. RNA expression analysis of FSHR and c-Myc proteins in OAW42 and in OVCAR3 cells respectively with/without treatment with active fraction F4 of MRE by semiquantitative RT-PCR method (E, F). The band intensities of each gene were normalized to GAPDH gene in both cell lines, using Biorad Image lab software (E, F). For semiquantitative RT-PCR in OAW42 and OVCAR3 respectively, a fold change of ≤ 1.2 was considered significant. * indicate statistical significance ($p \leq 0.05$) (G, H, Supplementary Table S5B).

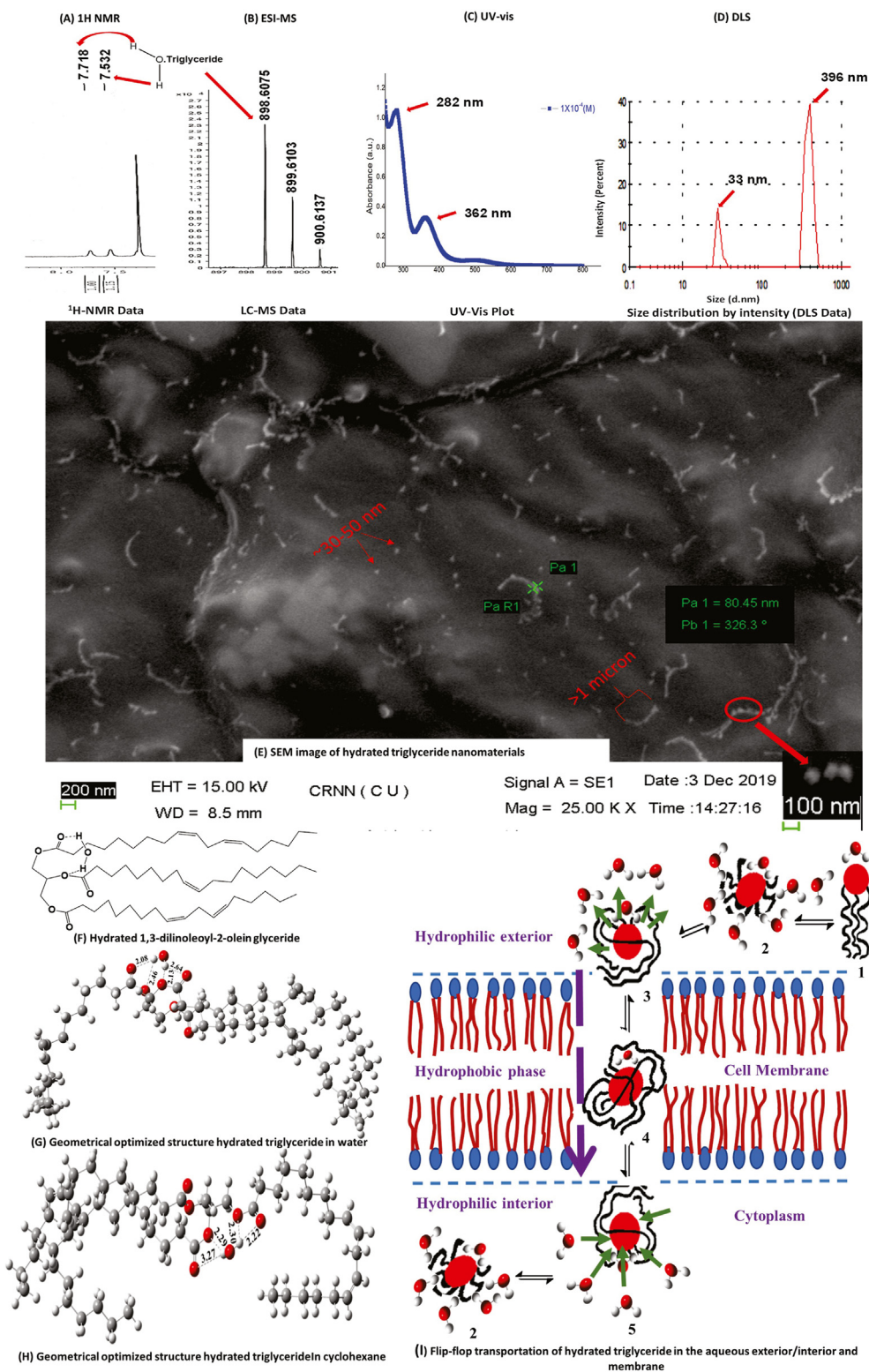


Fig. 5. Characterization, nano-scale property, transportation, and DFT study of hydrated-triglyceride. (A) ¹H NMR spectrum of the drug with chemically two non-equivalent protons. (B) ESI-MS spectrum of water bound drug. (C) UV-vis and (D) DLS spectrum. (E) SEM image of the as-extracted drug after sample preparation by spin coating method. Optimized geometrical morphology of the drug in water (F) and cyclohexane (G). (H) Model for easy transportation of the hydrated-triglyceride through the aqueous exterior, interior and lipophilic cell membrane.

semiquantitative RT-PCR. TR and RB conducted the Western blot experiments. Experimental design for in vivo experiment was made by RB. The in vivo experiment was conducted by RB, AG and PD. The article was drafted by RB, CKB and DKM. AG, RN and SM worked for purification of active compound from MRE. DKM identified the active compound and deduced its properties. AM, KC, SC provided essential workspace, laboratory and interactive support. RM and NG helped in DFT calculations.

Funding

We acknowledge Indian Council of Medical research for funding the project entitled “Role Of Moringa oleifera Lam. Root In Breast Cancer And Epithelial Ovarian Cancer Cell Line” to Dr Chinmoy K Bose, principal investigator of the project (Memo No: 59/54/2011/BMS/TRM) and providing the fellowship to Mr Arijit Ghosh. We acknowledge funding for DBT-SyMeC project (No. GAP357) and University Grant Commission (Memo No: 22/12/2013 (ii) EU-V) for providing fellowship to Ms Tanaya Roychowdhury. We acknowledge University Grant Commission for providing the fellowship (Memo No: F.15-6 (DEC2013)/2014 (NET)) to Mr Chandraday Prodhan.

Declaration of competing interest

The authors declare that they have no known competing financial interests or personal relationships that could have appeared to influence the work reported in this paper.

The authors declare that they have no known competing financial interests or personal relationships that could have appeared to influence the work reported in this paper.

Acknowledgments

General: We acknowledge Dr Aparna Khanna, NMIMS, Mumbai for providing OAW42 cell line and Dr Asima Mukhopadhyay, Chittaranjan National Cancer Institute, Kolkata for OVCAR3 cell line. We acknowledge Miss Arunima Dutta, Netaji Subhas Chandra Bose Cancer Research Institute, for her help regarding mice maintenance. We acknowledge Dr. Krishna Das Saha, Cancer Biology and Inflammatory Disorder Division, Indian Institute of Chemical Biology.

Funding: We also acknowledge Mr Tapan Halder, Department of Pathology, Netaji Subhas Chandra Bose Cancer Research Institute, for facilitating bulk tissue block preparation. We acknowledge Mr Tanmoy Dalui, Technical Operator of BD LSR Fortessa and Ms Debalina Chakraborty, Technical assistant of flow cytometry facility, Indian Institute of Chemical Biology and Mr. George Banik, Application Specialist BD for their help with operating flow cytometer. We acknowledge Dr. Ashis Mukhopadhyay, Medical Director, Netaji Subhas Chandra Bose Cancer Research Institute for his immense help and support.

Appendix A. Supplementary data

Supplementary data to this article can be found online at <https://doi.org/10.1016/j.jtcme.2021.03.005>.

References

- Webb PM, Jordan SJ. Epidemiology of epithelial ovarian cancer. *Best Pract Res Clin Obstet Gynaecol.* 2017;41:3–14. <https://doi.org/10.1016/j.bpobgyn.2016.08.006>.
- Koshiyama M, Matsumura N, Konishi I. Recent concepts of ovarian carcinogenesis: type I and type II. *BioMed Res Int.* 2014;934261:1–11. <https://doi.org/10.1155/2014/934261>.
- Bose CK. Anomalous endocrine feedback of peri-menopause in the etiology of type II ovarian cancer. *Future Oncol.* 2013;9:1257–1261. <https://doi.org/10.2217/fon.13.147>.
- Choi JH, Choi KC, Auersperg N, Leung PC. Overexpression of follicle-stimulating hormone receptor activates oncogenic pathways in preneoplastic ovarian surface epithelial cells. *J Clin Endocrinol Metab.* 2004;89:5508–5516. <https://doi.org/10.1210/jc.2004-0044>.
- Omara T, Kiprop AK, Ramkat RC, et al. Medicinal plants used in traditional management of cancer in Uganda: a review of ethnobotanical surveys, phytochemistry, and anticancer studies. Evidence-Based Complementary and Alternative Medicine. *Evid Based Complementary Altern Med.* 2020;2020. <https://doi.org/10.1155/2020/3529081>.
- Lampronti I, Khan MT, Bianchi N, Vizzello L, Fabbri E, Gambari R. Bangladeshi medicinal plant extracts inhibiting molecular interactions between nuclear factors and target DNA sequences mimicking NF-kappaB binding sites. *Med Chem.* 2005;1:327–333. <https://doi.org/10.2174/1573406054368684>.
- Al-Asmari AK, Albalawi SM, Athar MT, Khan AQ, Al-Shahrani H, Islam M. Moringa oleifera as an anti-cancer agent against breast and colorectal cancer cell lines. *PLoS One.* 2015;10, e0135814. <https://doi.org/10.1371/journal.pone.0135814>.
- Berkovich L, Earon G, Ron I, Rimmon A, Vexler A, Lev-Ari S. Moringa Oleifera aqueous leaf extract down-regulates nuclear factor-kappaB and increases cytotoxic effect of chemotherapy in pancreatic cancer cells. *BMC Compl Altern Med.* 2013;13:212. <https://doi.org/10.1186/1472-6882-13-212>.
- Tiloke C, Phulukdaree A, Chuturgoon AA. The antiproliferative effect of Moringa oleifera crude aqueous leaf extract on human oesophageal Cancer Cells. *J Med Food.* 2016;19:398–403. <https://doi.org/10.1089/jmf.2015.0113>.
- Jung IL, Lee JH, Kang SC. A potential oral anticancer drug candidate, Moringa oleifera leaf extract, induces the apoptosis of human hepatocellular carcinoma cells. *Oncol Lett.* 2015;10:1597–1604. <https://doi.org/10.3892/ol.2015.3482>.
- Guon TE, Chung HS. Moringa oleifera fruit induce apoptosis via reactive oxygen species-dependent activation of mitogen-activated protein kinases in human melanoma A2058 cells. *Oncol Lett.* 2017;14:1703–1710. <https://doi.org/10.3892/ol.2017.6288>.
- Abd-Rabou AA, Abdalla AM, Ali NA, Zoheir KM. Moringa oleifera Root Induces cancer apoptosis more effectively than leave nanocomposites and its free counterpart. *Asian Pac J Cancer Prev APJCP.* 2017;18:2141–2149.
- Shukla S, Mathur R, Prakash AO. Antifertility profile of the aqueous extract of Moringa oleifera roots. *J Ethnopharmacol.* 1988;22:51–62. [https://doi.org/10.1016/0378-8741\(88\)90230-9](https://doi.org/10.1016/0378-8741(88)90230-9).
- Ray K, Hazra R, Guha D. Central inhibitory effect of Moringa oleifera root extract: possible role of neurotransmitters. *Indian J Exp Biol.* 2003;41:1279–1284.
- Bose CK. Possible role of Moringa oleifera Lam. root in epithelial ovarian cancer. *MedGenMed.* 2007;9:26.
- Yang X. Clonogenic assay to test cancer therapies. *Bio Protoc.* 2012;2:1–3. <http://www.bio-protocol.org/e187>.
- Franken NA, Rodermond HM, Stap J, Haveman J, van Bree C. Clonogenic assay of cells in vitro. *Nat Protoc.* 2006;1:2315–2319. <https://doi.org/10.1038/nprot.2006.339>.
- Sur S, Pal D, Banerjee K, et al. Amarogentin regulates self-renewal pathways to restrict liver carcinogenesis in experimental mouse model. *Mol Carcinog.* 2016;55:1138–1149. <https://doi.org/10.1002/mc.22356>.
- Perrone F, Suardi S, Pastore E, et al. Molecular and cytogenetic subgroups of oropharyngeal squamous cell carcinoma. *Clin Canc Res.* 2006;12:6643–6651. <https://doi.org/10.1158/1078-0432.ccr-06-1759>.
- Bhattacharya R, Mukherjee N, Dasgupta H, et al. Frequent alterations of SLIT2-ROBO1-CDC42 signalling pathway in breast cancer: clinicopathological correlation. *J Genet.* 2016;95:551–563. <https://doi.org/10.1007/s12041-016-0678-2>.
- Catteau-Jonard S, Jamin SP, Leclerc A, Gonzales J, Dewailly D, di Clemente N. Anti-Mullerian hormone, its receptor, FSH receptor, and androgen receptor genes are overexpressed by granulosa cells from stimulated follicles in women with polycystic ovary syndrome. *J Clin Endocrinol Metab.* 2008;93:4456–4461. <https://doi.org/10.1210/jc.2008-1231>.
- Doe MR, Ascano JM, Kaur M, Cole MD. Myc post-transcriptionally induces HIF1 protein and target gene expression in normal and cancer cells. *Cancer Res.* 2012;72:949–957.
- Li F, Cao L, Hang D, Wang F, Wang Q. Long non-coding RNA HOTTIP is up-regulated and associated with poor prognosis in patients with osteosarcoma. *Int J Clin Exp Pathol.* 2015;8:11414–11420.
- Marone M, Mozzetti S, De Ritis D, Pierelli L, Scambia G. Semiquantitative RT-PCR analysis to assess the expression levels of multiple transcripts from the same sample. *Biol Proced Online.* 2001;3:19–25.
- Jivrajani M, Shaikh MV, Shrivastava N, Nivsarkar M. An improved and versatile immune-suppression protocol for the development of tumor xenograft in mice. *Anticancer Res.* 2014;34:7177–7183.
- Zhao Y, Truhlar GD. Applications and validations of the Minnesota density functionals. *Chem Phys Lett.* 2011;502:1–13. <https://doi.org/10.1016/j.cplett.2010.11.060>.
- Frisch M, et al. *Gaussian 16*. Wallingford, CT: Gaussian, Inc.; 2016.
- Tomasi J, Mennucci B, Cammi R. Quantum mechanical continuum solvation models. *Chem Rev.* 2005;105:2999–3093. <https://doi.org/10.1021/cr9904009>.
- Nieburgs EH. *Nuclear/Cytoplasmic Ratio (N/C) and Nuclear Chromatin. Diagnostic Cell Pathology in Tissue and Smears*. New York & London: Grune and Stratton; 1967:15–16.

30. Ramsewak RS, Nair MG, Murugesan S, Mattson WJ, Zasada J. Insecticidal fatty acids and triglycerides from *Dirca palustris*. *J Agric Food Chem*. 2001;49:5852–5856. <https://doi.org/10.1021/jf010806y>.
31. Bekele B, Adane L, Tariku Y, Hailu A. Evaluation of antileishmanial activities of triglycerides isolated from roots of *Moringa stenopetala*. *Med Chem Res*. 2013;22:4592–4599. <https://doi.org/10.1007/s00044-013-0467-x>.
32. Menon U, Riley SC, Thomas J, et al. Serum inhibin, activin and follistatin in postmenopausal women with epithelial ovarian carcinoma. *BJOG*. 2000;107:1069–1074. <https://doi.org/10.1111/j.1471-0528.2000.tb11102.x>.
33. Bose CK, Menor U, Thomas JM, Dawnay AB, Jacobs IJ. Gonadotrophin levels in postmenopausal women with epithelial ovarian cancer. *J Obstet Gynaecol India*. 2001;51:147–149.
34. Bose CK. Role of nerve growth factor and FSH receptor in epithelial ovarian cancer. *Reprod Biomed Online*. 2005;11:194–197. [https://doi.org/10.1016/s1472-6483\(10\)60958-3](https://doi.org/10.1016/s1472-6483(10)60958-3).
35. Zheng W, Magid MS, Kramer EE, Chen YT. Follicle-stimulating hormone receptor is expressed in human ovarian surface epithelium and fallopian tube. *Am J Pathol*. 1996;148(1):47–53. [https://doi.org/10.1016/s1472-6483\(10\)60958-3](https://doi.org/10.1016/s1472-6483(10)60958-3).
36. Balamurugan S, Vijayakumar S, Prabhu S, Morvin Yabesh JE. Traditional plants used for the treatment of gynaecological disorders in Vedaranyam taluk, South India - an ethnomedicinal survey. *J Tradit Complement Med*. 2017;8:308–323.
37. Wei S, Lai L, Yang J, Zhuandi G. Expression levels of follicle-stimulating hormone receptor and implication in diagnostic and therapeutic strategy of ovarian cancer. *Oncol Res Treat*. 2018;41:651–654. <https://doi.org/10.1159/000490810>.
38. Kato A, Ando K, Tamura G, Arima K. Effects of some fatty acid esters on the viability and transplantability of Ehrlich ascites tumor cells. *Cancer Res*. 1971;31:501–504.
39. Miyake JA, Benadiba M, Colquhoun A. Gamma-linolenic acid inhibits both tumour cell cycle progression and angiogenesis in the orthotopic C6 glioma model through changes in VEGF, Flt1, ERK1/2, MMP2, cyclin D1, pRb, p53 and p27 protein expression. *Lipids Health Dis*. 2009;8:8. <https://doi.org/10.1186/1476-511x-8-8>.
40. Falconer JS, Ross JA, Fearon KC, Hawkins RA, O'Riordain MG, Carter DC. Effect of eicosapentaenoic acid and other fatty acids on the growth in vitro of human pancreatic cancer cell lines. *Br J Canc*. 1994;69:826–832. <https://doi.org/10.1038/bjc.1994.161>.
41. Dachev M, Bryndova J, Jakubek M, Moučka Z, Urban M. The effects of conjugated linoleic acids on cancer. *Processes*. 2021;9:454. <https://doi.org/10.3390/pr9030454>.
42. Xu Y, Qian SY. Anti-cancer activities of ω -6 polyunsaturated fatty acids. *Biomed J*. 2014;37:112–119. <https://doi.org/10.4103/2319-4170.131378>.